Self-Assembling Nanofibers from Thiophene–Peptide Diblock Oligomers: A Combined Experimental and Computer Simulations Study

Alexey K. Shaytan,[†,‡,▽,*] Eva-Kathrin Schillinger,[§,▽,*] Pavel G. Khalatur,[†,⊥] Elena Mena-Osteritz,[§] Jens Hentschel,[¶] Hans G. Börner,[¶] Peter Bäuerle,[§] and Alexei R. Khokhlov[†,#]

[†]Institute of Polymer Science, University of Ulm, Albert-Einstein-Allee 47, D-89069 Ulm, Germany, [‡]Faculty of Biology, Moscow State University, 119991 Moscow, Russia, [§]Institute of Organic Chemistry II and Advanced Materials, University of Ulm, Albert-Einstein-Allee 11, D-89081 Ulm, Germany, [⊥]Institute of Organoelement Compounds, Russian Academy of Science, 119991 Moscow, Russia, [¶]Department of Chemistry, Humboldt-Universität zu Berlin, Brook-Taylor-Strasse 2, D-12489 Berlin, Germany, and [#]Faculty of Physics, Moscow State University, 119991 Moscow, Russia. [▽]These two authors contributed equally to this work.

ABSTRACT We report herein the synthesis of a novel type of hybrid compound that consists of a poly(ethylene oxide) (PEO) functionalized β-sheet peptide sequence covalently linked to an alkylated quaterthiophene moiety. Compounds of this class are highly promising for technological applications because their self-assembly and stimuli-responsive behavior, which is mainly caused by the peptide moieties, combined with the potential semiconducting properties of oligothiophenes provides unprecedented opportunities for the design of advanced materials at the nanoscale in such areas as, for example, organic electronics and sensor design for chemical and biomedical applications. The compound presented herein is experimentally shown to form stable fibrillar aggregates that are visualized by both transmission electron and atomic force microscopy. We developed a theoretical methodology to study the possible intermolecular arrangements and their characteristic features with the help of all-atom MD simulations, while simultaneously incorporating available experimental data into the model. Large-scale atomistic simulations of several fibrillar aggregates with different molecular arrangements were performed. The results of the simulations are compared with experimental data, which leads to the proposition of a likely model for the arrangement of the individual molecules within the observed aggregates.

KEYWORDS: molecular dynamics simulations · nanoelectronics · oligothiophenes · peptides · polymer bioconjugates · self-assembly

Hybrids between oligothiophenes and peptides present a promising approach toward the design of self-assembling functional π-systems. Owing to electron delocalization and thus π-conjugation, polythiophenes belong to the class of conductive polymers ("synthetic metals").[1] The (semi) conducting, optical, and electroluminescent properties of polythiophene derivatives combined with facile processing techniques (compared to that of solid-state semiconductors) have drawn much attention in recent decades because of the many possible technological applications in fields such as organic electronics (including light emitting diodes,[2] flexible displays,[3] and photovoltaic cells[4]), sensor and biosensor design,[5,6] design of bioelectric interfaces,[7] and others. Covalent attachment of functional groups to thiophene moieties may influence the structural and electronic properties of thiophenes, which are known to depend on ordering effects on both the molecular and the nanoscale level.[8]

Polymer–bioconjugates are macromolecules that consist of synthetic polymer blocks covalently linked to biological (macro)molecules such as peptides, nucleotides, and saccharides. These hybrid materials are either designed to benefit from the synergistic behavior of both components or to overcome shortcomings inherent to one component alone. Recent progress in the field of bioconjugate design, synthesis, and functions has been comprehensively summarized, and highlights the structure–property relationships of functional hybrid block copolymers.[9–15] The conjugation of oligothiophenes and biological macromolecules may result in new compounds that supplement the potentially semiconducting, optical, and electroluminescent properties of oligo- and polythiophenes with the self-assembling, specific binding, and stimuli-responsive behavior of biological moieties, thus opening opportunities for the design of smart materials and molecules at the nanoscale. Moreover the conjugation with biological moieties adds the new "biological" paradigm of using multiple levels of structure to create diversity of function out of simple, universal elements to synthetic chemistry.[16] Current research trends include the design of self-assembling

* Address correspondence to alexey.shaytan@uni-ulm.de, eva.schillinger@uni-ulm.de.

Received for review March 30, 2011 and accepted August 8, 2011.

Published online August 08, 2011
10.1021/nn2011943

oligothiophene "nanowires",[17−19] chemical and biological sensors with specific binding,[20] and bioelectrical interfaces, *etc*.

To date, hybrids of oligothiophenes with nucleotides,[21,22] single amino acids,[23] peptides,[17−19] and sugars[24] have been synthesized. The dominant factors responsible for self-assembly of such hybrid compounds are the hydrogen-bonding patterns of the biological moieties that are determined by the sequence of their building blocks and usually dominate the resulting nanostructure.[25] Owing to the relatively weak nature of hydrogen bonding, the resulting interplay of intermolecular interactions (H-bonding, van der Waals interactions, and $\pi-\pi$-stacking) also suggests the dependence of the supramolecular organization on the external conditions (such as temperature, solvent quality, pH value, *etc*); therefore, these hybrids are promising for technological applications.[26]

In the design of polymer-peptide conjugates, one of the most promising approaches is to use peptides with a β-sheet secondary structure motif,[27] because these peptides are known for their strong intermolecular aggregation. An inspiration for such systems comes partially from natural amyloid-like fibrils (involved also in a number of diseases such as Alzheimer's disease, type 2 diabetes, Huntington's disease, and Creutzfeldt-Jacob's disease[28]), which are formed because of the aggregation of certain protein sequence fragments into a cross-β-sheet quaternary structure, in which the β-sheet runs perpendicular to the fibril axis.[29] These fragments are typically 8−16 amino acids in length, and have an alternating sequence of hydrophobic and hydrophilic amino acids that forms a bilayer of β-sheet tapes with either the hydrophilic or the hydrophobic side chains buried between the tapes. These remarkably ordered and stable filamentous aggregates can be useful as building blocks for protein-based functional nanomaterials (amyloid fibrils are among the stiffest biological materials known to date, with a Young's modulus up to 20 GPa).[30−33]

The few examples of biohybrids that combine oligothiophenes and β-sheet-forming amino acid sequences have been reported only recently. We have synthesized a T-P type molecule[18] where a regioregular 3-hexylquaterthiophene (T) is functionalized with the pentapeptide sequence Gly-Ala-Gly-Ala-Gly (P), known to form β-sheet domains in silkworm silk. We have also carried out investigations on a symmetrically substituted alkylated quaterthiophene-peptide hybrid (P-T-P) that comprises two β-sheet-forming sequences, $(Val\text{-}Thr)_3$.[19] Diegelmann et al.[17] have reported the successful synthesis of a bithiophene incorporated into a β-sheet-forming peptide sequence (Ala-Phe-Glu-Gln-Gln-bithiophene-Glu-Phe-Ala-Gln-Glu; P-T-P type hybrid). Two more examples of oligothiophene peptide hybrids were introduced by Stupp and co-workers. Initially, an amphiphile-based terthiophene hybrid that incorporates one glutamic acid and two alanine building blocks was presented.[34] This approach was extended in the following to two derivatives of a central quinquethiophene symmetrically substituted with two Lys-Lys-Leu-Leu sequences.[35] In all cited studies, the self-assembly of the presented hybrids has been visualized through atomic force (AFM), scanning tunneling (STM), or transmission electron microscopy (TEM); it was shown that under certain conditions, the oligothiophene-peptide-hybrids can self-assemble into long morphologically similar fibrillar aggregates (micrometer range).

However, the direct structure of the self-assemblies on a molecular level could not yet be probed, although different models are hypothesized.[17,19,36] Computer simulations provide the important possibility of shedding some light on the possible supramolecular organization patterns, their stability and the governing interplay of intermolecular interactions. To the best of our knowledge, our group was the first to apply the rational principles of structure prediction by using conformation space search, based on molecular mechanics, and subsequent molecular dynamics simulations to study the peptide-directed noncovalent assembly of thiophene-peptide conjugates.[36−39] Gus'kova *et al*. recently summarized the possible models of fibrils formed from conjugates of alkylated quaterthiophenes with silk-inspired Gly-Ala-Gly-Ala-Gly sequences[36] (see also a recent review[40]).

Herein we report the synthesis of a new compound, a PEO-functionalized alkylated quaterthiophene-β-sheet-peptide diblock oligomer, which is experimentally shown to self-assemble into fibrillar aggregates in organic solvent. The core idea behind such a synthesis is to obtain molecular structures capable of self-assembly into filaments at the nanoscale level that would potentially be electrically (semi)conductive and at the same time would have high tensile strength as observed in natural amyloid and silk fibers.[30] We supplement the experimental findings with atomistic computer simulations (molecular dynamics) of possible supramolecular organization patterns for the observed aggregates and deduce the atomistic model for the arrangement of the molecules in the observed fibrils. A new theoretical/simulations approach is used which consists of (i) constructing the possible intermolecular arrangements consisted with experimental data, (ii) deriving all-atom models of fibrillar aggregates from these arrangements, and (iii) subsequent analysis by large scale molecular dynamics simulations. The main focus of the work presented herein is hence to explicitly describe the complex self-assembly process of a novel oligothiophene−peptide hybrid by the help of an unprecedented combined in-depth experimental and theoretical approach.

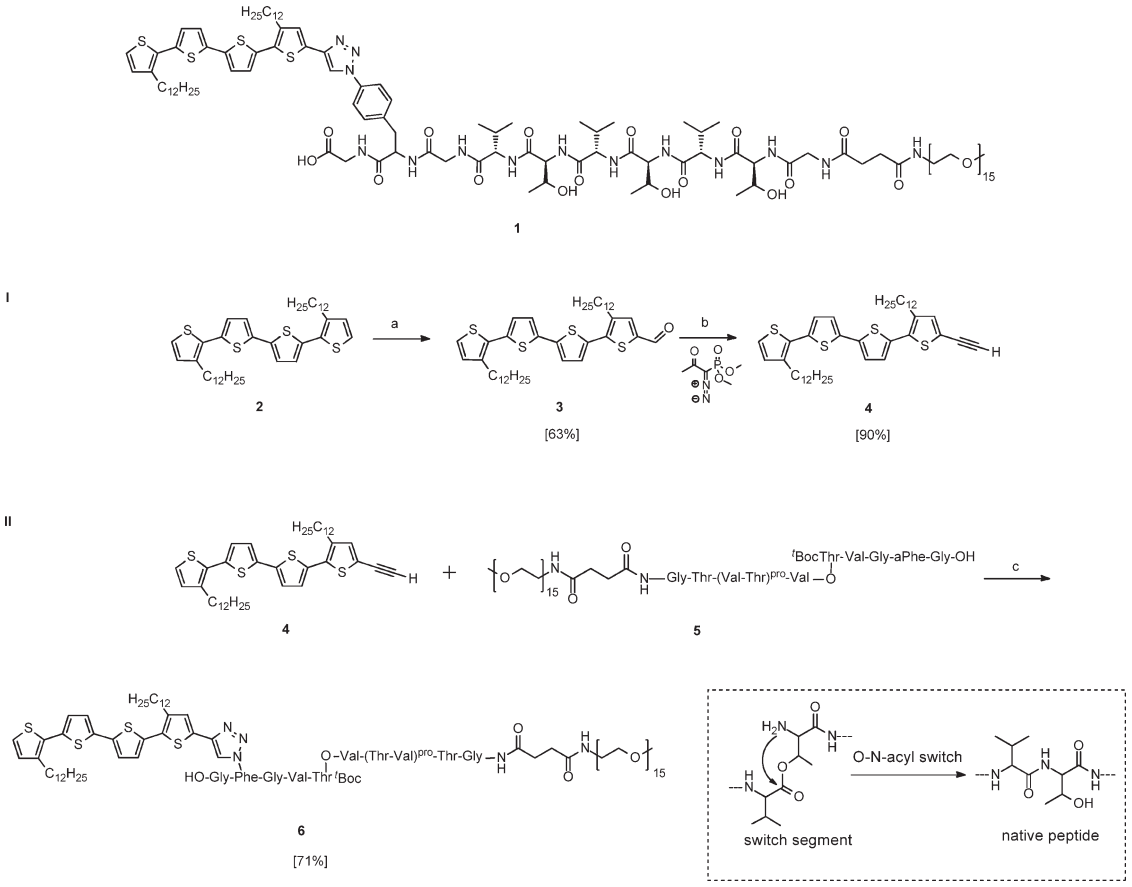

Scheme 1. Structure of quaterthiophene–β-sheet–peptide hybrid 1 and synthesis of precursor 6; (a): $POCl_3$, DMF, dichloroethane, reflux, 3h; (b): K_2CO_3, methanol/THF, room temp, overnight; (c): $[Cu(CH_3CN)_4]PF_6$, Cu°, DCM, room temp, 24 h. $(Thr\text{-}Val)^{pro}$ refers to a pseudoproline unit, (Val-O-Thr) refers to the switch unit, and aPhe stands for *p*-azido-Phe.

RESULTS AND DISCUSSION

Synthesis. T-P hybrid compound **1** (Scheme 1) was designed by the combination of a symmetrically didodecyl-substituted quaterthiophene that is functionalized on one side with a PEO–β-peptide conjugate. The sequence of the peptide comprises three repeats of Val and Thr. The quaterthiophene employed has been shown previously to self-assemble into highly regular superstructures at the liquid–solid interface (STM) and in the bulk (X-ray diffraction, XRD).[41–43] $(Val\text{-}Thr)_x$ repeats are known to form stable β-sheets in aqueous and organic media.[44–46]

Such β-sheet forming sequences are known as "difficult sequences"[47,48] because they tend to aggregate during synthesis and workup. Herein, two strategies were pursued to circumvent such unwanted aggregation and in addition to gain control over the self-assembly process. First, a so-called pseudoproline unit was incorporated into the peptide, which upon acidic deprotection is converted into a Val-Thr repeat.[49] Second, a switch ester moiety was utilized that produces a temporary defect in the native amide backbone by introduction of a β-ester connectivity between Val^5 and Thr^6.[50–52] The switch defect is preserved under acidic conditions, but the native amide backbone can be re-established by an increase in pH, thus triggering a rearrangement in the switch ester unit (O→N-acyl transfer, inset Scheme 1). The introduction of a para-azido-phenylalanine (*a*Phe) defines the ligation site in a side chain of the peptide and enables the attachment of the quaterthiophene by Cu(I)-catalyzed Huisgen cycloaddition, which proved to be very useful for peptide conjugation because of its high chemoselectivity and synthetically quantitative character.[53,54] For better flexibility of the resulting hybrid, a potentially secondary-structure-breaking glycine was introduced between the para-azido-phenylalanine and the β-sheet sequence. Eventually, the hybrid was equipped with a PEO chain at the N-terminus in order to enhance solubility and to prevent potential lateral interactions of fibrillar aggregates.

PEO–peptide–quaterthiophene precursor **6** was synthesized starting from symmetrically didodecyl-substituted quaterthiophene **2**[42] (Scheme 1,I). Vilsmeier–Haack formylation of **2** with phosporylchloride and *N*,*N*-dimethyl-formamide (DMF) gave monoaldehyde **3** in 63% yield. **3** was converted into the monoethynylated species **4** under Ohira–Bestman conditions.[55–59] The desired product **4** was obtained in 90% yield. Ligation of freshly prepared **4** with the PEO–peptide conjugate **5** was accomplished by Cu(I)-catalyzed Huisgen

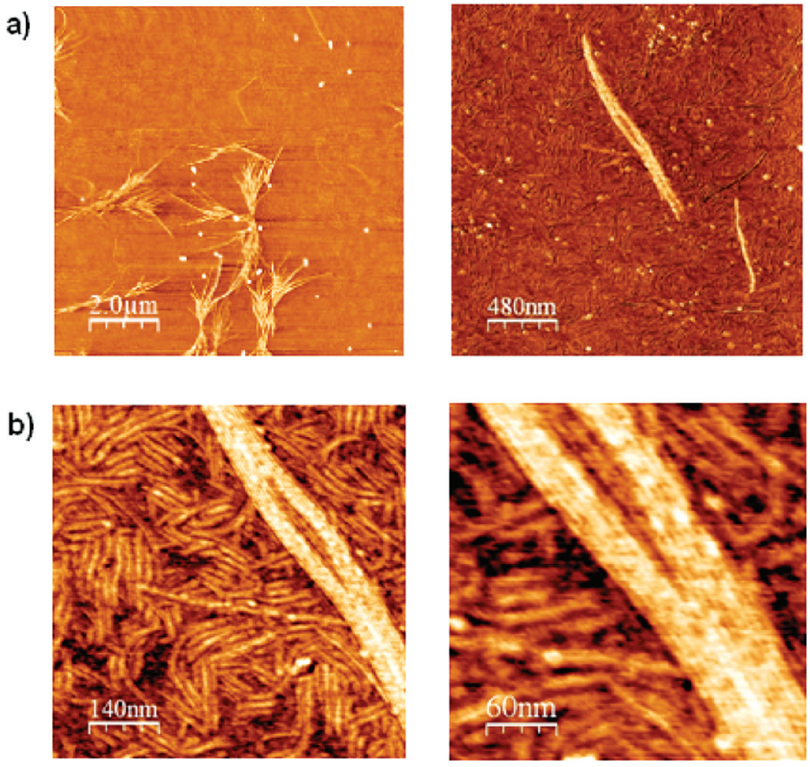

Figure 1. AFM height and phase images of native PEO–peptide–quaterthiophene 1, spincoated on mica from a DCM/0.001 M NaOH in MeOH solution 1:1 prepared by syringe pump: (a) AFM height images of (left) fiber bundles obtained after 7 days and (right) single fiber; (b) AFM phase images, (left and right) zoom of single fiber, showing the composition of the bigger fiber from small filaments.

cycloaddition, tetrakis(acetonitrile)copper(I) hexafluorophosphate was used as catalyst (Scheme 1,II).[60] The reaction was complete after 24 h and the crude product was purified by size exclusion chromatography (SEC) with tetrahydrofuran (THF) and subsequent precipitation with diethyl ether from dioxane. After drying in vacuum, fully protected PEO–peptide–quaterthiophene hybrid **6** could be isolated as an orange compound in 71% yield.

The compound was characterized by ^{1}H NMR spectroscopy, which confirmed the overall stoichiometry of one quaterthiophene building block to one peptide–PEO hybrid (see the Supporting Information, Figure S1). Owing to aggregation tendencies of T-P system **6**, for ^{1}H NMR analysis elevated temperatures and a mixture of deuterated solvents became necessary (77 °C, $C_2D_2Cl_4$/MeOH-d_4 3:1). Matrix assisted laser desorption ionization time-of-flight (MALDI-TOF) spectra revealed two homologous series with 44 Da mass difference of the PEO repeat units, each ($m/z_{(\text{max intensity})}$ = 2661.9 and 2678.1, which can be assigned to $[M + Na]^+$ and $[M + K]^+$, respectively, with 15 ethylene glycol repeat units and an end group mass of 1260.75 Da). Analytical gel permeation chromatography (GPC) for compound **6** was indicative of higher molecular weight than for the pure peptide–PEO hybrid **5** (see the Supporting Information, Figure S2). For deprotection, **6** was treated with 30% trifluoroacetic acid (TFA) in dichloromethane. Under these acidic conditions, all protecting groups present in hybrid **6** (^{t}Boc, pseudoproline, ^{t}butyl-ester) are removed, except for the switch ester segment, which is preserved. Thus, the molecule still exhibits a kink (**7**, see the Supporting Information for structure, Figure S3) in the peptide backbone.

To promote the conversion of the disturbed peptide segments of hybrid **7** into native β-strands (**1**), a controlled approach was chosen by the addition of 0.001 M sodium hydroxide dissolved in methanol to a previously prepared solution of **7** in dichloromethane (DCM) by a syringe pump, until a solvent ratio of 1:1 was reached (solvent-guided strategy, see below: 0.001 M NaOH in MeOH 0 vol % → 50 vol % in 12 h). The presence of the fully extended β-sheet sequence was proven by IR spectroscopy (see the Supporting Information, Figure S4). In the FT-IR spectrum, the absence of the bands for the intact switch ester moiety (ν = 1785 cm^{-1} and ν = 1743 cm^{-1}) accompanied by a shift of the amide I band to a region specific for β-sheet secondary structure (ν = 1636 cm^{-1}) indicates the presence of a fully extended peptide structure in **1**, which is engaged in the formation of a β-sheet secondary structure (see the Supporting Information, Figure S4). For a better comparison, the carbonyl region of the FT-IR spectrum of **7** is given as well. Because of the rather broad shape of the amide I band for hybrid **1** in a β-sheet secondary structure, it was

unfortunately impossible to unambiguously determine whether an antiparallel (specific band at $\nu = 1690\ cm^{-1}$) or a parallel orientation (lack of this band) of the peptide strands is present in the β-sheet.[60]

Self-Assembly. For the unsymmetrical PEO–β-peptide–oligothiophene hybrid **1**, self-assembly on the surface and in solution was investigated. Taking into account the different polarities of the hybrid (dominating hydrophobic interactions on the part of the oligothiophene, hydrogen bonding of the peptide segment) and the strong aggregation tendencies of the β-sheet peptide in its native form, a solvent-guided strategy utilizing a syringe pump was chosen for the simultaneous rearrangement of the peptide backbone and the self-assembly of hybrid **1** (see above).[19]

With the help of AFM, fibers were detected in a spincoated sample of **1** on a muscovite mica substrate (Figure 1). The images were obtained in tapping mode after stabilization of the adsorbate for several days. An accumulation of fibers could be visualized, the pattern of which does not correspond to a network but is more reminiscent of clusters (Figure 1a, left). Surrounding these larger areas of concentrated material, single "bigger" fibers can be found (Figure 1a, left and right). It could be shown that these single bigger fibers are bundles of several thinner fibers of different length aligned in parallel (Figure 1b, both images), which explains the irregularly frayed appearance of the bigger single fibers, which we therefore refer to as bundles. Furthermore, short fibrillar structures that surround the bundles are deposited regularly on the mica surface (Figure 1b). These short fibrillar structures can be considered to represent the smallest single structures, which then hierarchically self-assemble into bigger structures (bundles or even clusters).

The size of the bundles disperses between lengths of 1 to 2 μm, heights of 1 ± 0.2 nm and widths of 15–48 nm, although also sporadic widths of up to approximately 80 nm could be observed. The smallest self-assembled unit on the mica substrate (the aforementioned short fibrillar structures that are presumably single-layered β-sheets, see further discussion) show lengths of 100–500 nm and repeated widths of 7 ± 2 nm and heights of 0.5 ± 0.2 nm. The inconsistencies of the dimensions for the bundles, especially the width, are considered to be a result of a proposed hierarchical self-assembly that leads from single β-sheets (smallest observed fibrillar features) to double tapes, that is double-layered β-sheets (single fibers within a bundle), which in turn laterally interact to form bundles (see "Proposed Molecular Organization" subsection for further discussion).

In transmission electron microscopy (TEM), structures very similar to the ones investigated by AFM were observed (see the Supporting Information, Figure S5). A network structure of very long fibers that shows a broad width distribution can be clearly recognized (Figure S5, right). It is striking, that the fibers visualized in TEM seem to have a much longer persistence length than the ones observed in AFM. This result could be attributed to the higher concentration of the solution used for TEM investigations. It is much more likely, though, to be caused by the differing sample preparations (AFM, spin-coating; TEM, drop-casting), most notably the forces that act on the self-assembled structures during sample preparation.

Since the fibrillar objects could be observed by AFM on mica after spin-coating and also in TEM after drop-casting on carbon-coated copper grids, it can be assumed that these nano- and microstructures are already present in solution, and predominant effects of the substrates on the self-assembly are unlikely.[19] As was mentioned before, also the quaterthiophene part in the hybrid presented here is able to self-assemble by π–π stacking and van der Waals interactions.[41–43] Hence, the potential role of π–π interactions in the final self-assembled suprastructure was investigated by UV–vis, fluorescence, and CD spectroscopy.

To be able to compare the effects in self-assembled fibers to the nonassembled compound, two different solutions were prepared for investigation. The first sample (A, see the Supporting Information, Figure S6a), was prepared by slow addition of 0.001 M NaOH in methanol to a DCM solution of the quaterthiophene–peptide hybrid **1** by a syringe pump, as described above, and the second one (B, Figure S6b) by directly dissolving the kinked precursor compound 7 in a 1:1 mixture of methanol and DCM, thus leaving the peptide segment in a kinked state and hence hindering self-assembly. For both ways of preparing the sample, a gradual change in concentration over 2 orders of magnitude did not cause any changes in either position ($\lambda_{max} = 394 \pm 1$ nm) or shape of the π–π^* transition band, which can be seen from the normalized absorption spectra (Figure S6).

The absorption spectra for B (see Figure S6b), though, reveal that in the region of the π–π^* transition and the n–π^* transition of the kinked peptide (λ = 190–220 nm), which is partially overlapped with the region of the excitation of the oligothiophene part perpendicular to the long axis of the molecule, an increase in intensity of the band with decreasing concentration occurs. This behavior most likely has to be attributed to the influence of the peptide absorption bands, thus suggesting that the disturbed peptidic moieties of the hybrid interact with one another in a nonspecific manner at higher concentrations while they exist molecularly dissolved at lower concentrations. The effect of band broadening, which is observed for the highest concentration employed in the normalized absorption spectra for case A (Figure S6a) of preparing aggregation samples of **1**, is assigned to interactions between the single fibrous aggregates, which with growing concentration in the solution leads to scattering effects and thus unspecific broadening of all absorption bands.

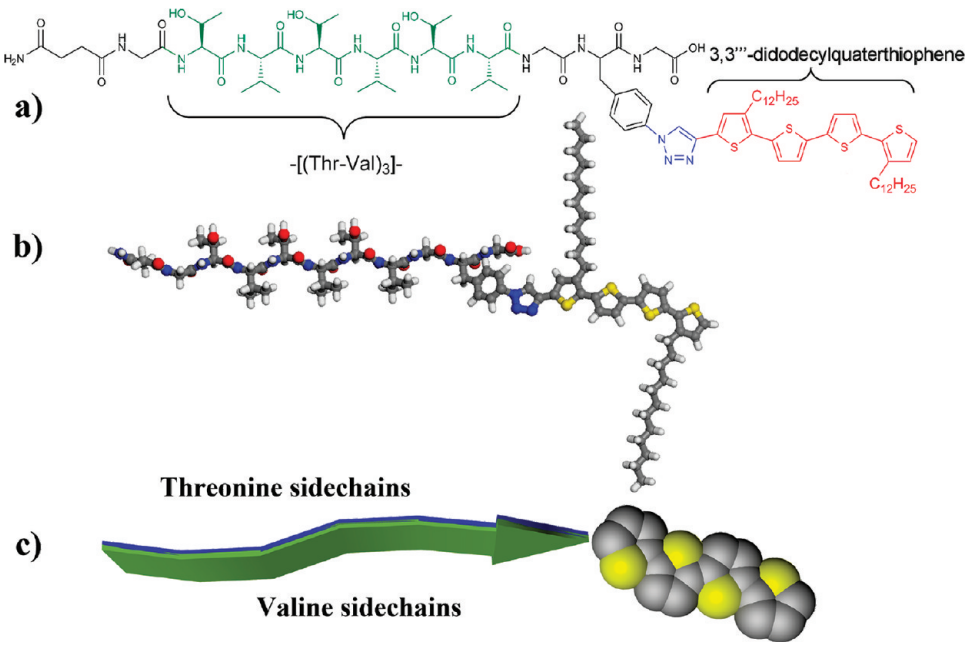

Figure 2. Various representations of the molecule used for computer simulations of self-assembling fibrillar aggregates: (a) structural formula, (b) all-atom representation with backbone conformation corresponding to that of the β-strand, (c) schematic representation of the β-strand and the quaterthiophene moiety.

Fluorescence spectroscopy, as a very sensitive method, did not reveal any aggregation that directly affects the π-system (see the Supporting Information, Figure S7). From CD spectroscopy, no indication of a chiral excitonic coupling of the conjugated π-systems of the quaterthiophenes could be obtained. However, a very weak nonbisignated signal in the CD spectrum at energies lower than the absorption maximum of the conjugated π-system points to the existence of chromophore aggregates in a chiral environment (see the Supporting Information, Figure S8a, green circle). When the normalized absorption spectra of the nonaggregated hybrid (kinked state of the peptide, **7**) and the aggregated sample (native state of the peptide, **1**) are compared, here, too, differences in the same region of the spectra become apparent (see the Supporting Information, Figure S8b): the sample prepared by slow addition of 0.001 M NaOH in methanol to a dichloromethane solution of the compound, which gives the native state of the peptide and thus leads to β-sheet formation (red line), exhibits a tailed absorption between 450 and 600 nm (green circle in Figure S8b). These results are hypothesized to be caused by the arrangement of the chromophore backbones in J-type aggregates in a chiral environment, which could easily overcome distances beyond the ideal ones for efficient exciton coupling interactions and for which a nonbisignated chiral signature may be detectable by CD spectroscopy.[61]

Models of Intermolecular Arrangements. As a starting point for the theoretical considerations of the experimentally observed nanofibers, the molecular structure of the oligothiophene–peptide hybrid as depicted in Figure 2 was chosen, and a corresponding all-atom molecular mechanics model was constructed. The model compound differs from the experimental one by the absence of the flexible PEO tail, since the PEO tail does not dispose of the ability for defined intermolecular interactions and initially was mainly added for solubility reasons. Therefore, at our level of simulations methodology, the PEO chains are unlikely to play an important structure-determining role.

Unfortunately, *ab initio* atomistic simulations of the complete self-assembly process for the molecular system under study are far beyond modern computational capabilities, which are generally limited to simulation times in the nanoseconds range while self-assembly happens on larger time scales. Hence, to apply atomistic simulations to gain insight into the structure, properties, and governing intermolecular interactions in such systems, a separate methodology that combines simulation techniques with available experimental data and rational understanding of the interactions hierarchy in self-assembly should be applied. Herein we demonstrate such a methodology developed to study the fibrillar aggregates from polymer bioconjugates (further details with respect to the theoretical research methodology workflow can be found in the Supporting Information).

In principle both parts of the hybrid molecule (conjugated part and peptide part) are capable of strong intermolecular interactions, thus leading to the formation of highly anisotropic structures such as nanofibers, nanorods, *etc.* As the formation of fibers at the nanoscale (especially amyloid-like fibers) from β-sheet

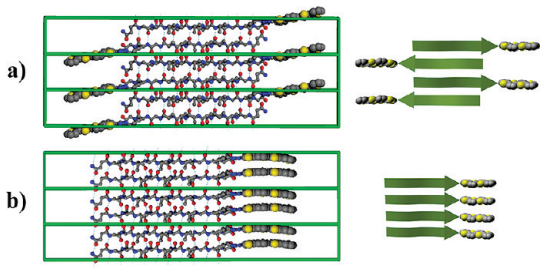

Figure 3. Constructed periodic crystalline cells for (a) antiparallel and (b) parallel arrangement of peptide strands in single-layer fibrils. Alkyl chains were omitted for clarity; dashed lines represent the hydrogen bonds responsible for β-sheet formation. Right insets show the principal arrangement of peptide and thiophene moieties.

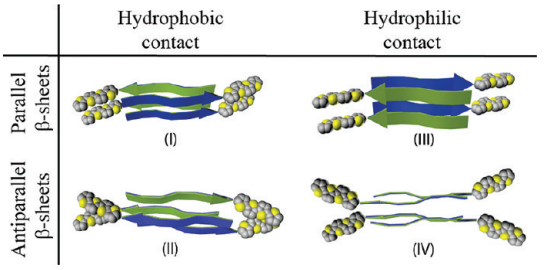

Figure 4. Schematic representations of constructed double-layer periodic arrangements from the hybrid molecule 1 classified by β-sheet orientation (parallel or antiparallel) and the type of β-sheet interlayer contact (hydrophobic, valine−valine; hydrophilic, threonine−threonine).

peptides is a common self-assembly mechanism,[62] similar peptide−peptide interactions may play the structure-determining role for suprastructure formation of our hybrid compound.

The majority of the experimental data available in literature (including X-ray and NMR-spectroscopy-resolved structures of amyloid-like fibrils) suggest that in biological amyloid fibers, the main structural aggregation motif of the peptides is the formation of long β-sheet tapes by laterally interacting single peptide β-strands. These tapes may in turn stack on top of each other face-to-face to form fibrils (filaments) with the so-called cross-β-spine quaternary structure that is considered to be the main characteristic feature of amyloid fibrils. Stacks of the tapes may further interact with each other and form thicker filamentous aggregates.[63] However, if the face-to-face interactions between tapes are hindered, the tapes may curl into helical structures as proposed by Aggeli *et al*. based on their theoretical models supported by experimental observations[63] and also found in congener PEO−peptide or poly(butylacrylate)−peptide or poly(butadien)−peptide conjugates.[64,65] The preference for parallel or antiparallel β-sheet arrangements in such fibrillar structures is disputable. Although many experimentally investigated amyloid-like fibrils were found to have a parallel β-sheet arrangement, different amyloid fibrils that may be astonishingly similar in coarse structural design, can vary substantially in molecular details, including the parallel or antiparallel arrangement of β-sheets.[66]

Starting from the above-mentioned ideas related to the structural organization of peptide molecules into filamentous aggregates, we propose several periodic arrangements for our hybrid compound, based on the assumption that the peptide part of the compound is organized in a similar manner. Two proposed basic periodic arrangements comprise an either parallel or antiparallel organization of the peptide moieties in the β-sheets. Another four arrangements were derived from these single layer arrangements by stacking the β-sheets face-to-face in an aggregation manner similar to the cross-β-spine structure of amyloid fibrils. Two basic single-layer periodic arrangements based on parallel and antiparallel β-sheets were constructed according to Material and Methods using the combination of molecular alignment and molecular dynamics simulations and are depicted in Figure 3. The obtained single-layer periodic structures were then used as building blocks to form various double-layer structures. We constructed these double-layer arrangements from the equilibrated single-layer dimers, striving to mimic the arrangement of the peptide part seen in amyloid-like fibrillar structures resolved by XRD or NMR spectroscopy[29,67] followed by an extensive relaxation MD simulation run that allows the molecules to adjust their periodic arrangement to the best local minimum of free energy.

The double-layer arrangements were created as follows: the single-layer structure was replicated, turned 180° around the axis of the tape, and then adjusted in the lateral plane, so that the peptide segments of two single-layer fibrils would be approximately in register, thus forming the center of the hybrid fibril. The β-sheets within such a fibril can interact with either the valine side chains or the threonine side chains of each sheet facing each other. Any overlap of molecular fragments that occurred (*e.g.*, within alkyl chains) was solved by small adjustments of the involved torsion angles that would anyway obtain their equilibrium values during the relaxation run. The discussed procedure resulted in four different double-layer periodic systems presented in Figure 4. In principle, for the parallel arrangement of the β-strands, another two double-tape conformations with reduced symmetry may be thought of when the β-strands in both tapes run parallel to each other. However, such structures were considered to be unlikely since (i) such a structural arrangement of β-strands was not observed experimentally to date for biological amyloid fibers, (ii) such an arrangement will not be favored by the interaction of dipole moments of the adjacent tapes, and (iii) only one such arrangement is sterically allowed because of the bulkiness of the thiophene fragments of the hybrid molecule.

Since double layers are considerably more complex conformational assemblies, particularly with respect to

the organization of the surfaces buried between the two β-sheets and the interaction of the side chains at these surfaces, a 10 ns molecular dynamics (MD) relaxation run was performed for these periodic structures. During this run, a certain rearrangement of the side chain conformations between the β-sheets took place (for details of the MD simulation see the Supporting Information). The relative enthalpies of formation for all structures during the run were monitored: the lowest enthalpy of formation being observed for structure III (*i.e.*, the most energetically favorable structure). With respect to structure III, structures I, II, and IV were less energetically favorable and had higher values of enthalpies of formation by 11, 6, and 12 kcal/mol per molecule, respectively (statistical error: 1−2 kcal/mol). Although this data set was obtained in vacuum simulations and the effect of solvent was neglected, it gives valuable quantitative data for the understanding of the hierarchy of interactions in such systems and is consistent with the hypothesis that hydrophilic interlayer contacts and an antiparallel arrangement of the β-sheets are the factors that lead to a gain in enthalpy of formation. However, in our case because of the specific geometry of the molecules, the aggregation pattern based on antiparallel β-sheets and hydrophilic interlayer contact (see Figure 4, system IV) leads to the loss of close packing between the thiophene moieties and thus becomes energetically unfavorable. Owing to the specificity of the attachment of the thiophene moiety to the peptide, a closer packing may only be achieved by conformational changes of the peptide backbone, which, however, leads to less efficient interactions between peptide strands in the β-sheet.[68]

Fibril Simulations. Both obtained single-layer periodic arrangements and two of the double-layer structures were used to construct long fibrils by replicating the periodic cell along the axis of the filament. Among the double-layer structures, arrangements II and III were chosen for further study since they (i) are the arrangements with the lowest enthalpies of formation among others and (ii) represented two different basic kinds of arrangement with either parallel or antiparallel stacking of β-strands, which should allow interesting comparative analysis of the influence of parallel or antiparallel arrangement patterns on the fiber morphology and evolution. For the selected systems, planar straight fibrils of 80 β-strands in length (approximately 40 nm) were constructed and subjected to 10 ns MD simulations at T = 300 K. Additionally, for comparative analysis, simulations of fibrils that consist of the pure peptide backbone were conducted. The initial structures for pure peptide fibrils were derived from the original fibrils by deleting the alkylated thiophene moiety together with the triazolyl linker and by reconstruction of the phenylalanine side chain by addition of a hydrogen atom. The length of the fibrillar aggregates was chosen large enough to avoid the influence of possible "edge" effects on the overall conformation of the aggregates (which for congener amyloid fibrils may be estimated in the order of 10 nm[69]) on one hand and computational tractability on the other hand. The lengths of the fibrillar aggregates used in the state of the art works on all-atom simulations of amyloid fibrils, which is believed to allow tracing their geometric characteristics, is around 20−30 nm.[31,70]

Large-scale MD simulations were performed in parallel on 64 CPUs. The number of atoms in the simulated systems ranged approximately from 20 to 40 thousand atoms. To this end, the LAMMPS simulation package[71] based on the domain decomposition strategy was employed (for further simulation details see the Supporting Information).

Conformational Evolution. The conformational evolution of the constructed aggregates during the simulations allows both the study of the shape and morphology of the fibrils and also the tracing of the influence of the intermolecular arrangement on the conformation of the aggregates at the nanoscale. Comparative analysis of various fibrils (including the all-peptide fibrils) allows us to discuss the role of various intermolecular interactions in stability and behavior of the aggregates.

A comprehensive list of snapshots that describe the conformational evolution of different fibrillar arrangements is presented in Figure 5 (the arrangements are in the following referred to as "a", "b", "c", and "d"). Although all systems demonstrated their stability during the simulation run, that is, all molecules preserved their relative positions in the aggregates with respect to their neighbors, conformational rearrangements both at the molecular level and at the nanoscale level were observed. In all cases, the β-sheet organization dominated the structure and remained the main scaffold for the fibril organization (see also further discussion). Ten nanosecond simulation times were enough to grasp the main characteristics of the fibril morphology and its evolution (bending, twisting, collapsing, *etc.*). As seen from Figure 5 panels a and b, the single-layer fibrils are capable of a more pronounced conformational rearrangement than double-layer fibrils, since the double-layer organization of the fibrils rigidifies them.

The simulations of single-layer fibrils with a parallel arrangement of β-strands (Figure 5a) revealed the importance of both thiophene−thiophene and peptide−peptide interactions for stability and rigidity of this type of fibrils. The fibril mainly remains rather linear and axially rigid, unlike its all-peptide counterpart (Figure 5a3) that tends to collapse into a more compact structure. The initially planar structure of the hybrid fibril undergoes certain twists with respect to its axis, while the peptide backbone conformation changes. As seen from Figure 5a2 the originally flat peptide sequences of the molecules have adopted a kinked appearance by rotational rearrangement of the

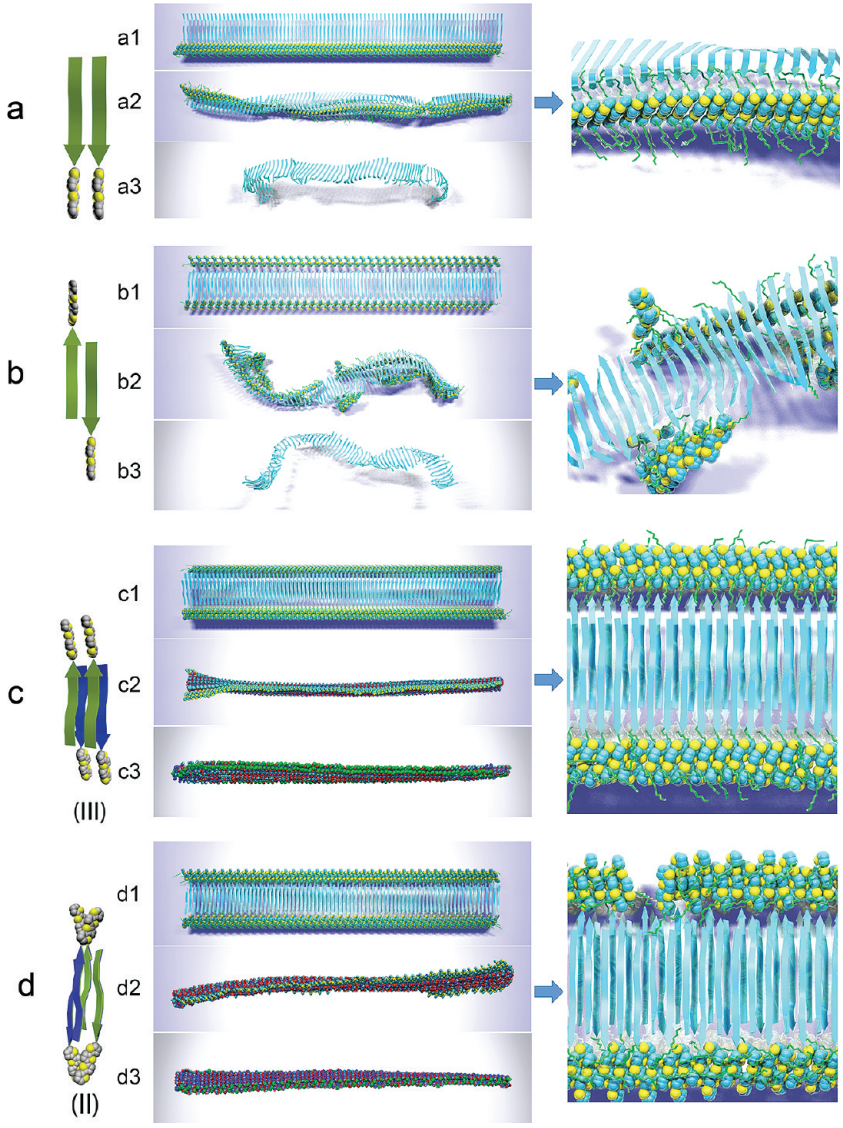

Figure 5. Simulation snapshots of four different types of fibrils. Initial conformation = a1, b1, c1, d1; after 10 ns of evolution = a2, b2, c2, d2; final snapshots for the evolution of the all-peptide fibrils = a3, b3, c3, d3. (Right) Enlarged snapshots corresponding to images a2, b2, c2, d2. Peptide moieties are depicted with arrows, thiophene moieties using van der Waals spheres, alkyl chains with green tubes. Images c2, c3, d2, d3 use van der Waals representation also for the peptide part for clarity.

peptide backbone at the position of the conformationally flexible glycine residue that connects the $(Thr-Val)_3$ sequence with the rest of the molecule. The thiophene moieties of the molecules, however, remain in closely packed alignment, thus forming a continuously organized axial structure with a left-handed twist. In contrast, the single-layer fibril based on the antiparallel arrangement of β-strands, which lacks much of the thiophene–thiophene interactions (because the spacing between the thiophene segments is twice as large as in the case of the parallel arrangement) tends to curl into a more tightly wound left-handed helical structure (Figure 5b). The thiophene moieties exist in a more disordered state than in an a-type fibril; however, their presence greatly changes the helical pitch and diameter of the helical structure when compared to all-peptide fibrils (Figure 5b3). As depicted on the large inset in Figure 5b, the thiophene moieties tend to form separated clusters along the tape of the fibril. Solvent effects may play a considerable role for the curling of the helix; it should depend on the balance between the interactions of the side chains on each side of the tape with each other as well as with the solvent. In our simulations, the fibril composed of the hybrid molecules (Figure 5b2) tended to have the hydrophobic face of the tape at the inner part of the helix while the all-peptide fibril adopted the opposite conformation (the hydrophilic threonine residues in this case have more opportunities for polar interactions and hydrogen bonding). The other curling conformation of the hybrid fibril is attributed to the position of the alkylated thiophene

moieties relative to the β-sheet plane. Additional possibilities for the oligothiophenes to saturate their steric contacts by packing more closely on the hydrophobic side of the tape result from the covalent attachment of the peptide moiety to the thiophene ring that bears an alkyl side chain pointing to the hydrophobic face of the fibril (see Figure 2b). Consequently these possibilities for close packing outweigh the competing possibilities for hydrophilic interactions of the threonine residues on the other face of the fibril.

Contrary to the single-layer fibrils, double-layer fibrils based on the arrangements c and d, that is, III and II in Figure 4, result in almost planar tapes with a possible twist along the axis. The interactions between the adjacent single-layer tapes through hydrogen bonding and steric interactions strengthen the structure and molecular order and also hinder peptide flexibility, thus disfavoring additional peptide bending, that is, kinks in single-layer fibrils (see above and Figure 5a). Moreover, the stacking of two tapes with identical faces implies other "geometrical" considerations, such as suppression of helix formation (each tape taken separately would prefer to curl in the opposite direction than the adjacent tape and thus the "curling" tendency vanishes). The double-tape fibril composed of parallel β-sheets stacked with hydrophilic faces (Figure 5c) remained mainly planar with only a small left-handed twist distortion at one end of the fibril that may be attributed to the edge effects. The size of this distortion is around 5 nm, which may be an estimate of the length at which the edge effects protrude into the body of the fibril. Surprisingly, the all-peptide fibril (Figure 5c3) revealed a small right-handed twist of the tape plane along the axis of the fibril, whereas β-sheets in general are considered to tend to have a left-handed twist; this behavior, though, is generally more pronounced for the antiparallel arrangement of β-strands.[72] In our simulations (Figure 5a3), the single tape of parallel β-strands of the all-peptide hybrid did not reveal any twisted behavior. However, it is known that the twisting behavior of β-sheets is mainly accounted for by subtle interactions of the side chains within one strand;[72] these intrastrand interactions may be affected by the presence of juxtaposed and neighboring β-sheets that offer alternative possibilities for interstrand interactions (*e.g.,* hydrogen bonding through threonine residues), which may shift the subtle balance of interactions, thus favoring either direction of twisting.

The double-tape arrangements based on antiparallel β-sheets (Figure 5d) formed a relatively planar stable left-handed twisted tape with an approximate twist of 30 degrees per 40 nm. This conformational behavior roughly corresponds to that observed in the simulations of only the peptide part of the fibril (Figure 5d3). Unlike the model of oligothiophene–peptide fibrillar aggregates based on alternating blocks of oligothiophene and peptide moieties (the "alternating superpolymer model") studied by computer simulations earlier,[39] the torsion along this type of fibrillar aggregate is persistent, strongly correlated, and is little influenced by thermal fluctuations.

$\pi-\pi$ Stacking *versus* H-Bonding. With respect to applications, the arrangement of the conjugated thiophene moieties and the interplay between $\pi-\pi$ stacking and β-sheet formation is the most important aspect of the work presented herein. The spacing between the peptide strands imposed by the β-sheet structure corresponds to 4.8–5 Å, while the spacing between the π-conjugated planes of oligothiophenes for $\pi-\pi$ stacking interactions is estimated to ideally be around 3.3–3.5 Å;[73,74] hence, these interactions show competing behavior in terms of the periodicity implied during molecular aggregation. The analysis of histograms for the distribution of distances between the centers of mass of peptides and also between quaterthiophenes (Figure 6) clearly revealed the domination of the periodicity implied on the aggregates by the arrangement of the peptides into β-sheets for all types of simulated fibrils. Therefore, the thiophene moieties had to adopt the periodical arrangement settled by the peptides, which deviates from the ideal $\pi-\pi$ stacking distance. In the case of a parallel arrangement of the β-strands (see the large insets in Figure 5a,c) the thiophene moieties tilt synchronously, thus simultaneously preserving the high degree of ordering and fulfilling the periodicity restrictions implied by the β-sheets. In the case of the antiparallel arrangement, the proposed double-layer fibril (Figure 5d) in principle has the same linear density of quaterthiophenes along the fibril as in the case of fibrils with parallel arrangement, since the thiophene moieties from both tapes come in contact to form a "steric zipper" along each side of the double tape (oligothiophene moieties from both sides are in alternating contact). However, for the antiparallel arrangement, the thiophene parts tend to lean toward one another to form dynamic clusters with gaps between the individual clusters (see the large inset in Figure 5d); such an arrangement reduces the differences between the optimal interthiophene and interpeptide distances. On the other hand, because of this tendency to form dynamic clusters, the degree of long-range order in the oligothiophene arrangement is considerably lower for the fibrils with antiparallel arrangement than for the ones with parallel β-strands (see Figure 5b).

The degree of $\pi-\pi$ interaction between the adjacent thiophene rings is visualized by the plots that present the fraction of thiophene rings that have at least one neighboring ring closer than the specified distance (Figure 7). The distances between the centers of mass of thiophene rings that participate in a $\pi-\pi$ stacking interaction according to quantum chemistry calculations are approximately 3.8–3.9 Å[73,74] (this distance is somewhat larger than the before-cited ideal distance between the π-conjugated planes because the adjacent oligothiophenes in a stack are laterally

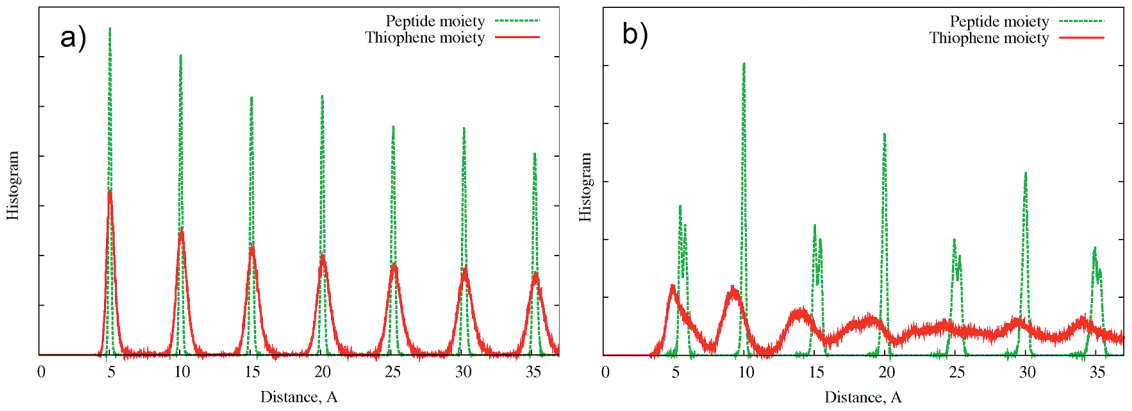

Figure 6. The plots present the distance distribution of peptide and thiophene blocks in the fibrils. All distances were calculated between the centers of mass of either peptide blocks or quaterthiophene blocks. (a) Fibril type c (double-layer tape with parallel arrangement of the β-strands); (b) fibril type d (double-layer tape with antiparallel arrangement of the β-strands). The peptide backbone periodicity in our model is roughly 5 Å and is remarkably conveyed to thiophene moieties in the case of type c fibrils.

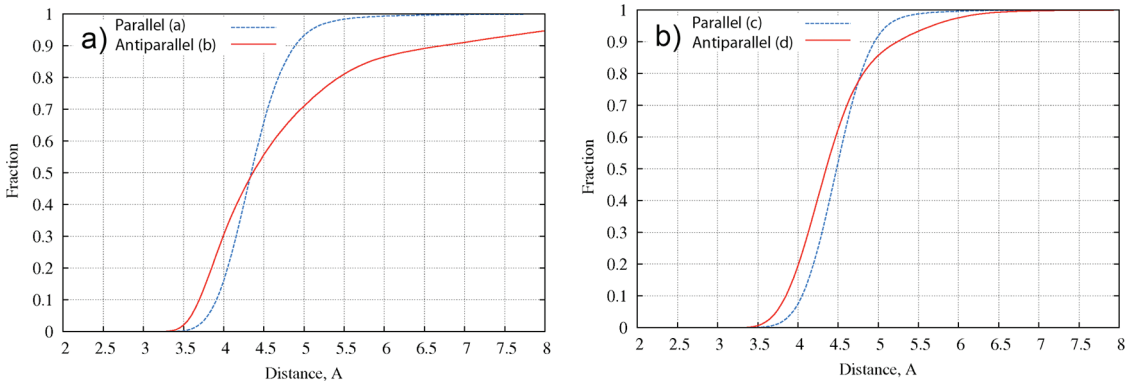

Figure 7. Fraction of thiophene rings in the entire fibril that have at least one other thiophene ring at a distance not greater than the abscissae values. Distances were measured between centers of mass of individual thiophene rings: (a) single-layer fibrils; (b) double-layer fibrils. Fibril types referring to Figure 5 are given in parentheses in the legend. The minimal interthiophene distance observed was 3.4 Å.

shifted). It is seen from the plots that for all different fibrils, only a minor fraction of rings complies with a $\pi-\pi$ stacking distance of not more than 3.9 Å. Although for both "antiparallel" fibrils, the fraction of rings that may participate in such "genuine" stacking interactions is around 20−30%, for both "parallel" fibrils, this fraction is significantly lower, being less than 5% in the case of the double-layer fibril.

Proposed Molecular Organization. As stated earlier and as supported by the data for congener peptide and polymer−bioconjugate systems,[65,75] molecular aggregation in our system is likely governed by a number of interactions of different nature and strength leading to a common hierarchical self-assembly pattern for β-sheet peptides: first the molecules assemble into β-sheet tapes, which then aggregate laterally to form double tapes (as in cross-β-structure of amyloid-like fibrils), which in turn form larger assemblies by various types of aggregation.

Available literature data suggest that self-assembly of polymer−bioconjugates based on similar β-sheet-forming peptides takes place already in solution,[75] and thus the structures observed at two different substrate surfaces deposited by either spin-coating (AFM, surface: mica) or drop-casting (TEM, surface: carbon-coated copper grids) should correspond to those prevalent in solution. It may be possible that the substrate exerts an influence on the orientation of the aggregates (especially smaller ones) or even their fragmentation, but it seems unlikely to be able to change the basic conformational features of the bigger fibrils formed in solution with large length to width ratio (such as twisted or helical organization), especially since the fibers visualized by both AFM and TEM were similar with respect to their inner architecture (see "Self-Assembly" subsection). It also seems to be a reasonable hypothesis that aggregates of different organizational levels (single tapes, double tapes, bundles of double tapes) may be present in solution at the same time in a dynamic equilibrium.

Judging by the characteristic height of the typically observed structures (see Figure 1) and in comparison with computational data (see discussion below), it may be proposed that the shortest fibrillar structures visible in the background of the AFM image correspond to single β-sheet tapes (with heights of 0.5 ± 0.2 nm,

Figure 5a1), while the bigger fibrils (with heights 1 ± 0.2 nm) are bundles of double tapes, in which the double tapes are organized according to Figure 5c. The structure of these double-layer fibers is of main interest.

AFM measurements of our fibrillar aggregates (Figure 1b) did not reveal any periodic height fluctuations along the fibrils, which are characteristic of twisted or helical structures and which are normally clearly resolved by AFM experiments.[19] Also in TEM, no indications for a helical superstructure of the fibers were found, thus we assume that the observed aggregates lack any twist or helical conformation.

Among the theoretical models for single β-sheet tapes (Figure 5a,b), both models manifested high conformational flexibility and small persistent lengths (compared to the double tape models), which is consistent with their behavior observed in AFM (as compared to the bigger fibers). It is hypothesized that for small single tapes the fast adsorption of the species on the substrate (here, mica) during sample preparation could make them adopt a planar conformation, which should be easier to accomplish for the fibrils with a parallel organization of β-strands (Figure 5a). The width of the smallest self-assembled fibrils measured in AFM is 7 ± 2 nm, which also nicely corresponds to the width of the type a fibril being in planar conformation. The fact that such smaller fibrils are not seen in TEM may again point to the assumption that the presence of such fibrils in AFM is due to kinetic reasons during sample preparation (single tapes are "trapped" on the substrate by fast adsorption).

As to the double-tape models, only the model based on a parallel arrangement of β-strands (Figure 5c) manifested the behavior free from substantial axial or helical twist observed in both AFM and TEM. In addition, the double-layer fibers are more rigid than the single-layer aggregates, thus a flattening of the double-layer structures helped by the surface (as was suggested for the single-layer structures) is unlikely. Hence we can conclude that from the results of our theoretical calculations the most plausible model for the organization of the structural elements of the observed bigger fibrils is that hybrid molecules aggregate into parallel β-sheets to form tapes and these tapes then further aggregate to form double-layer structures by interaction of their respective faces to gain additional stability and prevent curling and twisting as observed in Figure 5 panels a2 and b2. Which of the faces of the single-layer β-sheets would interact face-to-face with one another would depend on many factors including the solvent properties. The proposed intertape aggregation in model c (Figure 5) may therefore not be ultimately justified, but seems plausible to form in solvents of low polarity, in which polar and electrostatic interactions dominate the aggregation.

In the obtained CD and fluorescence spectra there was no sign for an excitonic coupling of the π-systems, which should occur with $\pi-\pi$ stacking in a chiral

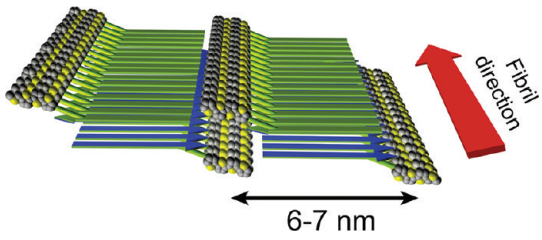

Figure 8. Proposed schematic model for the likely arrangement of hybrid molecules in the observed nanofibers consisting of smaller fibrils. β-Strands are depicted by green and blue arrows, quaterthiophenes are depicted by van der Waals spheres. Alkyl and PEO chains are omitted for clarity, and the peptide organization was simplified by using ideally planar β-pleated sheets.

environment at close to ideal $\pi-\pi$ stacking distances of the π-conjugated backbones. Among the theoretically studied models, type c also corroborates these experimental findings the best, because it has the lowest number of thiophene rings that are in close contact with one another (see Figure 7b) as compared to other models. Moreover, in the suggested arrangement type, the hitherto neglected flexible PEO tails of the molecules that are positioned in neighboring β-sheets may further interfere with the ordered arrangement of the thiophene moieties in the adjacent β-sheet and thus hinder the direct interaction of the π-systems; the PEO chains can even be hypothesized to interact with the energy levels of the π-systems.[19] On the other hand, the interaction of π-systems of thiophene moieties at distances greater than those characteristic for ideal $\pi-\pi$-stacking would be in accordance with the suggested interactions over greater distances (see the results form CD spectroscopy). Such "long-range" interactions might be accomplished in molecular assemblies similar to J-type aggregates with an arrangement of the hybrid molecules based on double layers of parallel β-sheets (Figure 8).

The hypothesized arrangement would also account for the composition of the bigger fibers/bundles from smaller fibrils observed in AFM and TEM (see Self-Assembly subsection). The proposed lateral aggregation of the double-tape fibrils into bundles as seen in Figure 8 could stem from microphase-separation tendencies of the system with van der Waals, hydrophobic, or hydrophilic interactions being the main forces active.

To visualize and further study the proposed molecular arrangement model, we performed MD simulations of the type c fibril on graphite and constructed a model of the AFM image based on the atomistic structure of such a systems (see Figure 9, for simulation details see the Supporting Information). The resulting data were visualized by WSxM imaging software.[76] The total width of the fibril as measured by virtual AFM algorithm is around 10 nm (see Figure 9c), while the maximum height is around 1.7 nm. It should be noted that the actual profile of the fibril may depend on many factors (tip radius, cantilever rigidity, and amplitude,

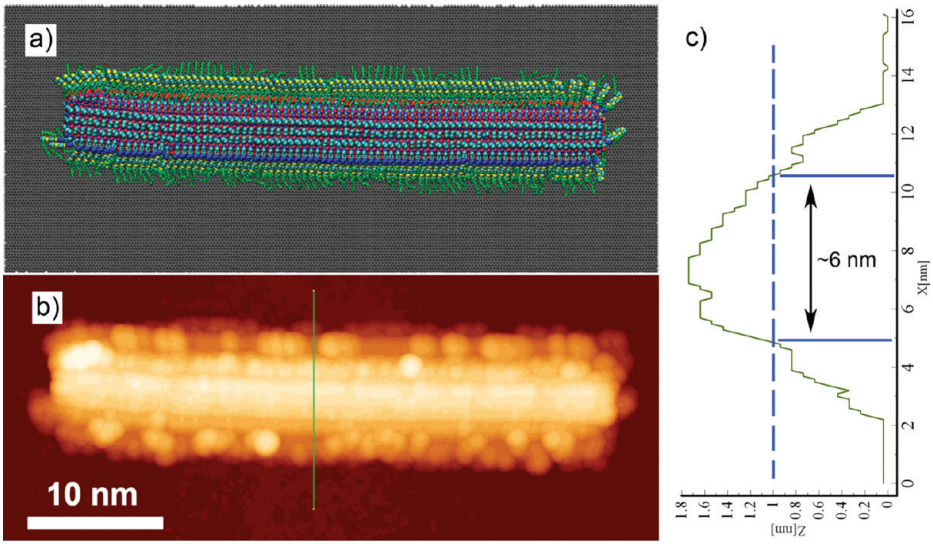

Figure 9. (a) Snapshot of an atomistic model of type c fibril adsorbed on graphite substrate after 10 ns MD simulations; (b) corresponding virtual AFM image; (c) height profile of fibril cross section marked in panel b with a green line. Blue lines in panel c present the suggested dimensions of the fibril in laterally aggregated bundle.

etc.), that is why in comparison with experimental data some reference structures should be considered. By the same virtual AFM technique, the maximum height of the single-layer fibril (type a) was estimated to be around 1 nm. The fact that the amino acid side chains of neighboring tapes efficiently pack at the interface of β-sheets contributes to the maximum height of the double layer structure being a little less than the sum of two single layer tapes (1.7 *vs* 2 nm). The computationally measured heights of the fibrils agree with that observed in AFM (1 ± 0.2 nm for the proposed double-tape structures and 0.5 ± 0.2 nm for the proposed single-tape structures) if taken comparatively: the height difference between single and double layer tapes is 0.5 ± 0.2 nm in AFM *versus* 0.7 ± 0.05 nm in simulation.

Since the fibrils depicted in Figure 9a are suggested to aggregate laterally in bundles (see Figure 8), one should consider that the AFM profile of fibrillar bundles would be 3different from the one depicted in Figure 9c, but rather have a bump-shaped periodic nature with a periodicity of approximately 6−7 nm and lower height fluctuations.

CONCLUSIONS

We reported the successful synthesis of a hybrid compound that consists of a PEO-functionalized peptide sequence with a high propensity to form β-sheets that are covalently linked to an alkylated quaterthiophene moiety. Compounds of this class are very promising for applications because their self-assembly and stimuli-responsive properties, provided by the peptide moieties, combined with the semiconducting properties of the thiophenes result in new opportunities for the design of smart materials at the nanoscale. The presented compound was experimentally shown to form stable fibrillar-like aggregates visualized by AFM and TEM. While the experimental evidence alone is not sufficient to reveal the exact molecular organization of such fibrils, a theoretical methodology was developed to study possible intermolecular arrangements and their characteristic features with the help of all-atom MD simulations. The methodology Zincorporated available experimental data to suggest different versions of possible fibrillar structures that were studied theoretically, and their behavior was then cross-validated against available experimental evidence. Large-scale all-atom MD simulations for several proposed fibrillar models were performed. They revealed the dependence of the fibrillar morphology on the intrinsic molecular organization of the fibrils. From the use of combined theoretical and experimental analysis, the most likely model of fibril formation and aggregation based on the parallel arrangement of the peptide strands into hierarchically further assembling β-sheets was suggested.

MATERIALS AND METHODS

Experimental Part. Details concerning the synthesis and characterization of the compounds can be found in the Supporting Information. Absorption spectra were recorded on a Perkin-Elmer Lambda 19 spectrometer and fluorescence emission spectra on a Perkin-Elmer LS 55 spectrometer in 1 cm cuvettes. FT-IR spectroscopy was performed on a Perkin-Elmer FT-IR Spectrum 2000 spectrometer, by using KBr pellets. Circular dichroism spectroscopy was performed on a *JASCO J-810* spectropolarimeter by using 2 mm cuvettes. Atomic force microscopy (AFM) was

performed on a MultiMode V device (Veeco Instruments, Santa Barbara, CA) in tapping mode by using standard phosphorus (n) doped silicon-cantilevers (spring constant: 40 N/m, frequency: 280 kHz). The images were recorded on a j-scanner. Samples were spin-coated (2500 rpm) from solution (0.12 mg/mL) on freshly cleaved mica substrates. Analyses of the aggregate dimension were carried out on a sample exhibiting separated structures by averaging over at least 25 values. Transmission electron microscopy (TEM) was carried out on a Zeiss EM 912Ω instrument at an acceleration voltage of 120 kV. The samples were drop-casted and then air-dried on carbon-coated copper grids. All reactions were performed in flame-dried glassware under argon and were monitored by thin layer chromatography (aluminum plates, precoated with silica gel, Merck Si60 F_{254}). Compounds were detected by UV and ninhydrin. Preparation of aggregation samples was as follows: A 0.5−0.53 mg portion of **6** was treated with 500 μL of 30% TFA for 3 h. Then the solvent was removed, and the sample was dried *in vacuo*. The residue (**7**) was redissolved in 500 μL of dichloromethane. To this solution, 500 μL of 0.001 M NaOH in methanol was added by syringe pump at a speed of 40 μL per hour. After the addition was finished, the sample was left to stand on a shaker for 7 d before spincoating.

Theoretical Models Construction. An all-atom molecular model of the compound under study was based on the Class II polymer-consistent force field (PCFF) with the parameters adjusted to reproduce the *ab initio* energy surfaces.[77−79] The total potential energy of the system is represented as a sum of the energy contributions of the following two categories: (i) valence terms, V_{val}, including the energy contributions for bond, angle, torsion, and out-of-plane angle coordinates as well as the energy contributions for diagonal and off-diagonal cross-coupling terms between internal coordinates; (ii) intra- and intermolecular nonbonded interaction terms, V_{nb}, which include a Lennard-Jones "9-6" potential for the van der Waals interactions and a Coulombic term for electrostatic interactions.

The construction of single layer periodic arrangements from single molecules was carried out with the inclusion of subsequent minimization and relaxation steps as follows. At first the conformations of the initial molecules were adjusted: the peptide block was considered to be in the form of a β-strand engaged in an ideal either parallel or antiparallel β-sheet that is solely determined by the values of the dihedral ϕ and ψ angles of the peptide backbone, which are known to be $\phi = -119°$, $\psi = 113°$ for peptide strands in parallel β-sheets and $\phi = -139°$, $\psi = 135°$ for peptide strands in antiparallel β-sheets.[70] The thiophene block including the 4-azidophenyl-alanine side chain and alkyl chains was considered to be in a planar, extended conformation that corresponds to the local energy minimum as depicted in Figure 3b. To obtain a proper periodic arrangement that could be used as an elementary structure to construct long fibrils, a corresponding periodic unit cell that consists of two (for single-layer fibrils) or four (for double-layer fibrils) molecules was derived. The period implied by the unit cell along the fibrillar axis was set to be 4.8 Å per β-strand as to correspond to the one generally observed in amyloid fibrils (9.6 Å for two strands).[80] As a first step, two molecules were arranged into two single-layered periodic structures with a parallel and an antiparallel arrangement of β-strands, the peptide segments in both cases were aligned as to maximize the number of interstrand hydrogen bonds (see Figure 3). Energy minimization for such periodic single-layer systems (that can be regarded as infinitely long crystalline tapes) was then performed followed by a relaxation MD simulation run of 1 ns.

Acknowledgment. Financial support from RFBR (projects 09-03-12033, 09-04-12146, 10-03-92003, and 10-04-01182), FTOP "Research and scientific-pedagogical staff of innovational Russia" for 2009-2013 (government Contract P475) and the Deutsche Forschungsgemeinschaft (SFB 569, project A11 "Self-organizing bioinspired oligothiophene-oligopeptide hybrids: A joint experimental and theoretical approach") is highly appreciated. The simulations were performed on a multiteraflop supercomputer SKIF at Moscow State University and on a SUN Fire cluster ALDAN at Ulm University.

Supporting Information Available: Experimental details including NMR spectra, GPC plots, FTIR-spectra, UV−vis absorption spectra, fluorescence emission spectra. Theoretical details including MD simulation protocols. This material is available free of charge *via* the Internet at http://pubs.acs.org.

REFERENCES AND NOTES

1. Schopf, G.; Kobmehl, G. *Polythiophenes—Electrically Conductive Polymers*; Springer: Berlin, 1997.
2. Garten, F.; Vrijmoeth, J.; Schlatmann, A.; Gill, R.; Klapwijk, T.; Hadziioannou, G. Light-emitting Diodes Based on Polythiophene: Influence of the Metal Workfunction on Rectification Properties. *Synth. Met.* **1996**, *76*, 85–89.
3. Choi, M.; Kim, Y.; Ha, C. Polymers for Flexible Displays: From Material Selection to Device Applications. *Prog. Polym. Sci.* **2008**, *33*, 581–630.
4. Cai, W.; Gong, X.; Cao, Y., Polymer Solar Cells: Recent Development and Possible Routes for Improvement in the Performance. *Sol. Energy Mater. Sol. Cells* **2009**.
5. Lange, U.; Roznyatovskaya, N.; Mirsky, V. Conducting Polymers in Chemical Sensors and Arrays. *Anal. Chim. Acta* **2008**, *614*, 1–26.
6. McQuade, T.; Pullen, A.; Swager, T. Conjugated Polymer-Based Chemical Sensors. *Chem. Rev.* **2000**, *100*, 2537–2574.
7. Widge, A.; Jeffries-El, M.; Cui, X.; Lagenaur, C.; Matsuoka, Y. Self-Assembled Monolayers of Polythiophene Conductive Polymers Improve Biocompatibility and Electrical Impedance of Neural Electrodes. *Biosens. Bioelectron.* **2007**, *22*, 1723–1732.
8. Sirringhaus, H.; Brown, P. J.; Friend, R. H.; Nielsen, M. M.; Bechgaard, K.; Langeveld-Voss, B. M. W.; Spiering, A. J. H.; Janssen, R. A. J.; Meijer, E. W.; Herwig, P.; *et al*. Two-Dimensional Charge Transport in Self-Organized, High-Mobility Conjugated Polymers. *Nature* **1999**, *401*, 685–688.
9. Börner, H. Strategies Exploiting Functions and Self-Assembly Properties of Bioconjugates for Polymer and Materials Sciences. *Prog. Polym. Sci.* **2009**, *34*, 811–851.
10. Gauthier, M.; Klok, H.-A. Peptide/Protein−Polymer Conjugates: Synthetic Strategies and Design Concepts. *Chem. Commun.* **2008**, 2591–2611.
11. Lutz, J.; Börner, H. Modern Trends in Polymer Bioconjugates Design. *Prog. Polym. Sci.* **2008**, *33*, 1–39.
12. Canalle, L.; Lowik, D.; Hest, J. Polypeptide−Polymer Bioconjugates. *Chem. Soc. Rev.* **2010**, *39*, 329–353.
13. Alemdaroglu, F.; Herrmann, A. DNA Meets Synthetic Polymers—Highly Versatile Hybrid Materials. *Org. Biomol. Chem.* **2007**, *5*, 1311–1320.
14. Börner, H.; Schlaad, H. Bioinspired Functional Block Copolymers. *Soft Matter* **2007**, *3*, 394–408.
15. Börner, H.; Kühnle, H.; Hentschel, J. Making "Smart Polymers" Smarter: Modern Concepts to Regulate Functions in Polymer Science. *J. Polym. Sci., Part A: Polym. Chem.* **2010**, *48*, 1–14.
16. Buehler, M. Tu(r)ning Weakness to Strength. *Nano Today* **2010**, *5*, 379–383.
17. Diegelmann, S.; Gorham, J.; Tovar, J. One-Dimensional Optoelectronic Nanostructures Derived from the Aqueous Self-Assembly of π-Conjugated Oligopeptides. *J. Am. Chem. Soc.* **2008**, *130*, 13840–13841.
18. Klok, H.-A.; Rösler, A.; Götz, G.; Mena-Osteritz, E.; Bäuerle, P. Synthesis of a Silk-Inspired Peptide-Oligothiophene Conjugate. *Org. Biomol. Chem.* **2004**, *2*, 3541–3544.
19. Schillinger, E.-K.; Mena-Osteritz, E.; Hentschel, J.; Börner, H.; Bäuerle, P. Oligothiophene *versus* β-Sheet Peptide: Synthesis and Self-Assembly of an Organic Semiconductor−Peptide Hybrid. *Adv. Mater.* **2009**, *21*, 1562–1567.
20. Mouffouk, F.; Brown, S.; Demetriou, A.; Higgins, S.; Nichols, R.; Rajapakse, G.; Reeman, S. Electrosynthesis and Characterization of Biotin-Functionalized Poly(terthiophene) Copolymers, and Their Response to Avidin. *J. Mater. Chem.* **2005**, *15*, 1186–1196.
21. Bäuerle, P.; Emge, A. Specific Recognition of Nucleobase-Functionalized Polythiophenes. *Adv. Mater.* **1998**, *10*, 324–330.

22. Jatsch, A.; Kopyshev, A.; Mena-Osteritz, E.; Bäuerle, P. Self-Organizing Oligothiophene-Nucleoside Conjugates: Versatile Synthesis *via* Click-Chemistry. *Org. Lett.* **2008**, *10*, 961–964.
23. Mucci, A.; Parenti, F.; Schenetti, L. A Self-Assembling Polythiophene Functionalised with a Cysteine Moiety. *Macromol. Rapid Commun.* **2003**, *24*, 547–550.
24. Schmid, S.; Mena-Osteritz, E.; Kopyshev, A.; Bäuerle, P. Self-Assembling Carbohydrate-Functionalized Oligothiophenes. *Org. Lett.* **2009**, *11*, 5098–5101.
25. Jatsch, A.; Schillinger, E.-K.; Schmid, S.; Bäuerle, P. Biomolecule Assisted Self-Assembly of Small π-Conjugated Oligomers. *J. Mater. Chem.* **2010**, *20*, 3563–3578.
26. Ikkala, O.; Brinke, G. Hierarchical Self-Assembly in Polymeric Complexes: Towards Functional Materials. *Chem. Commun.* **2004**, 2131–2137.
27. Vandermeulen, G.; Klok, H.-A. Peptide/Protein Hybrid Materials: Enhanced Control of Structure and Improved Performance through Conjugation of Biological and Synthetic Polymers. *Macromol. Biosci.* **2004**, *4*, 383–398.
28. Koo, E. H.; Lansbury, P. T.; Kelly, J. W. Amyloid Diseases: Abnormal Protein Aggregation in Neurodegeneration. *Proc. Natl. Acad. Sci. U.S.A.* **1999**, *96*, 9989–9990.
29. Nelson, R.; Sawaya, M.; Balbirnie, M.; Madsen, A.; Riekel, C.; Grothe, R.; Eisenberg, D. Structure of the Cross-[β] Spine of Amyloid-like Fibrils. *Nature* **2005**, *435*, 773–778.
30. Smith, J.; Knowles, T.; Dobson, C.; MacPhee, C.; Welland, M. Characterization of the Nanoscale Properties of Individual Amyloid Fibrils. *Proc. Natl. Acad. Sci. U.S.A.* **2006**, *103*, 15806–15811.
31. Paparcone, R.; Keten, S.; Buehler, M. Atomistic Simulation of Nanomechanical Properties of Alzheimer's Aβ(1−40) Amyloid Fibrils under Compressive and Tensile Loading. *J. Biomech.* **2010**, *43*, 1196–1201.
32. Knowles, T.; Oppenheim, T.; Buell, A.; Chirgadze, D.; Welland, M. Nanostructured Films from Hierarchical Self-Assembly of Amyloidogenic Proteins. *Nat. Nanotechnol.* **2010**, *5*, 204–207.
33. Cherny, I.; Gazit, E. Amyloids: Not Only Pathological Agents but Also Ordered Nanomaterials. *Angew. Chem., Int. Ed.* **2008**, *47*, 4062–4069.
34. Tsai, W.; Li, L.; Cui, H.; Jiang, H.; Stupp, S. Self-Assembly of Amphiphiles with Terthiophene and Tripeptide Segments into Helical Nanostructures. *Tetrahedron* **2008**, *64*, 8504–8514.
35. Stone, D.; Hsu, L.; Stupp, S. Self-Assembling Quinquethiophene−Oligopeptide Hydrogelators. *Soft Matter* **2009**, *5*, 1990–1993.
36. Gus'kova, O.; Khalatur, P.; Bäuerle, P.; Khokhlov, A. Silk-Inspired "Molecular Chimeras": Atomistic Simulation of Nanoarchitectures Based on Thiophene-Peptide Copolymers. *Chem. Phys. Lett.* **2008**, *461*, 64–70.
37. Gus'kova, O.; Khalatur, P.; Khokhlov, A. Molecular Chimeras: New Strategies in the Design of Functional Materials. *Nanotechnol. Russ.* **2008**, *3*, 481–493.
38. Gus'kova, O.; Schillinger, E.; Khalatur, P.; Bäuerle, P.; Khokhlov, A. Bioinspired Hybrid Systems Based on Oligothiophenes and Peptides (ALA-GLY)*n*: Computer-Aided Simulation of Adsorption Layers. *Polym. Sci., Ser. A* **2009**, *51*, 430–445.
39. Shaytan, A.; Khokhlov, A.; Khalatur, P. Large-Scale Atomistic Simulation of a Nanosized Fibril Formed by Thiophene−Peptide Molecular Chimeras. *Soft Matter* **2010**, *6*, 1453–1461.
40. Gus'kova, O.; Khalatur, P.; Khokhlov, A. Self-Assembled Polythiophene-Based Nanostructures: Numerical Studies. *Macromol. Theory Simul.* **2009**, *18*, 219–246.
41. Azumi, R.; Götz, G.; Debaerdemaeker, T.; Bäuerle, P. Coincidence of the Molecular Organization of β-Substituted Oligothiophenes in Two-Dimensional Layers and Three-Dimensional Crystals. *Chem.—Eur. J.* **2000**, *6*, 735–744.
42. Bäuerle, P.; Fischer, T.; Bidlingmeier, B.; Rabe, J. P.; Stabel, A. Oligothiophenes—Yet Longer? Synthesis, Characterization, and Scanning Tunneling Microscopy Images of Homologous, Isomerically Pure Oligo(alkylthiophene)s. *Angew. Chem., Int. Ed.* **1995**, *34*, 303–307.
43. Mena-Osteritz, E. Superstructures of Self-Organizing Thiophenes. *Adv. Mater.* **2002**, *14*, 609–616.
44. Janek, K.; Behlke, J.; Zipper, J.; Fabian, H.; Georgalis, Y.; Beyermann, M.; Bienert, M.; Krause, E. Water-Soluble β-sheet Models which Self-Assemble into Fibrillar Structures. *Biochemistry* **1999**, *38*, 8246–8252.
45. Hentschel, J.; Börner, H. G. Peptide-Directed Microstructure Formation of Polymers in Organic Media. *J. Am. Chem. Soc.* **2006**, *128*, 14142–14149.
46. Hentschel, J.; Krause, E.; Börner, H. Switch-Peptides to Trigger the Peptide Guided Assembly of Poly(ethylene oxide)-Peptide Conjugates into Tape Structures. *J. Am. Chem. Soc.* **2006**, *128*, 7722–7723.
47. Hentschel, J.; ten Cate, M. G. J.; Börner, H. G. Peptide-Guided Organization of Peptide−Polymer Conjugates: Expanding the Approach from Oligo- to Polymers. *Macromolecules* **2007**, *40*, 9224–9232.
48. Eckhardt, D.; Groenewolt, M.; Krause, E.; Börner, H. G. Rational Design of Oligopeptide Organizers for the Formation of Poly(ethylene oxide) Nanofibers. *Chem. Commun.* **2005**, 2814–2816.
49. Wöhr, T.; Wahl, F.; Nefzi, A.; Rohwedder, B.; Sato, T.; Sun, X.; Mutter, M. Pseudo-prolines as a Solubilizing, Structure-Disrupting Protection Technique in Peptide Synthesis. *J. Am. Chem. Soc.* **1996**, *118*, 9218–9227.
50. Sohma, Y.; Sasaki, M.; Hayashi, Y.; Kimura, T.; Kiso, Y. Novel and Efficient Synthesis of Difficult Sequence-Containing Peptides through O−N Intramolecular Acyl Migration Reaction of O-Acyl Isopeptides. *Chem. Commun.* **2004**, 124–125.
51. Mutter, M.; Chandravarkar, A.; Boyat, C.; Lopez, J.; Dos Santos, S.; Mandal, B.; Mimna, R.; Murat, K.; Patiny, L.; Saucède, L.; *et al.* Switch Peptides *In Statu Nascendi*: Induction of Conformational Transitions Relevant to Degenerative Diseases. *Angew. Chem., Int. Ed.* **2004**, *43*, 4172–4178.
52. Carpino, L. A.; Krause, E.; Sferdean, C. D.; Schümann, M.; Fabian, H.; Bienert, M.; Beyermann, M. Synthesis of Difficult Peptide Sequences: Application of a Depsipeptide Technique to the Jung-Redemann 10- and 26-mers and the Amyloid Peptide A[β](1−42). *Tetrahedron Lett.* **2004**, *45*, 7519–7523.
53. Lutz, J.-F.; Börner, H. G.; Weichenhan, K. Combining ATRP and "Click" Chemistry: A Promising Platform Towards Functional Biocompatible Polymers and Polymer Bioconjugates. *Macromolecules* **2006**, *39*, 6376–6383.
54. Lutz, J.-F.; Börner, H. G.; Weichenhan, K. Click Bioconjugation of a Well-Defined Synthetic Polymer and a Protein Transduction Domain. *Aust. J. Chem.* **2007**, *60*, 410–413.
55. Ghosh, A. K.; Bischoff, A.; Cappiello, J. Asymmetric Total Synthesis of the Gastroprotective Microbial Agent. *Eur. J. Org. Chem.* **2003**, *2003*, 821–832.
56. Krämer, C. S.; Müller, T. J. J., Synthesis and Electronic Properties of Alkynylated Phenothiazines. **2003**, 3534−3548.
57. Müller, S.; Liepold, B.; Roth, G. J.; Bestmann, H. J. An Improved One-Pot Procedure for the Synthesis of Alkynes from Aldehydes. *Synlett* **1996**, 521–522.
58. Ohira, S. Methanolysis of Dimethyl (1-Diazo-2-oxopropyl) Phosphonate: Generation of Dimethyl (Diazomethyl) Phosphonate and Reaction with Carbonyl Compounds. *Synth. Commun.* **1989**, *19*, 561–564.
59. Roth, G. J.; Liepold, B.; Müller, S. G.; Bestmann, H. J. Further Improvements of the Synthesis of Alkynes from Aldehydes. *Synthesis* **2004**, 59–62.
60. Aucagne, V.; Leigh, D. A. Chemoselective Formation of Successive Triazole Linkages in One Pot: "Click-Click" Chemistry. *Org. Lett.* **2006**, *8*, 4505–4507.
61. Lewis, F. D.; Liu, X.; Wu, Y.; Zuo, X. Stepwise Evolution of the Structure and Electronic Properties of DNA. *J. Am. Chem. Soc.* **2003**, *125*, 12729–12731.
62. Ecroyd, H.; Carver, J. Crystallin Proteins and Amyloid Fibrils. *Cell. Mol. Life Sci.* **2009**, *66*, 62–81.

63. Aggeli, A.; Nyrkova, I. A.; Bell, M.; Harding, R.; Carrick, L.; McLeish, T. C. B.; Semenov, A. N.; Boden, N. Hierarchical Self-Assembly of Chiral Rodlike Molecules as a Model for Peptide OI-Sheet Tapes, Ribbons, Fibrils, and Fibers. *Proc. Natl. Acad. Sci. U.S.A.* **2001**, *98*, 11857–11862.
64. Hentschel, J.; Börner, H. G. Peptide-Directed Microstructure Formation of Polymers in Organic Media. *J. Am. Chem. Soc.* **2006**, *128*, 14142–14149.
65. Jahnke, E.; Severin, N.; Kreutzkamp, P.; Rabe, J. P.; Frauenrath, H. Molecular Level Control over Hierarchical Structure Formation and Polymerization of Oligopeptide−Polymer Conjugates. *Adv. Mater.* **2008**, *20*, 409–414.
66. Margittai, M.; Langen, R. Fibrils with Parallel In-Register Structure Constitute a Major Class of Amyloid Fibrils: Molecular Insights from Electron Paramagnetic Resonance Spectroscopy. *Q. Rev. Biophys.* **2008**, *41*, 265–297.
67. Lührs, T.; Ritter, C.; Adrian, M.; Riek-Loher, D.; Bohrmann, B.; Döbeli, H.; Schubert, D.; Riek, R. 3D Structure of Alzheimer's Amyloid-β(1−42) Fibrils. *Proc. Natl. Acad. Sci. U.S.A.* **2005**, *102*, 17342–17347.
68. Several additional trial structures (data not shown) based on structure IV were analyzed, in which a distorted conformation of the peptide (the corresponding peptide backbone torsion angles were rotated) was used to arrange thiophene moieties in a closer contact. However, because of the energy penalty that originates from the distorted peptide conformation (hydrogen bond loss) none of the trial structures occurred to be more energetically favorable than the ones presented in Figure 4.
69. Xu, Z.; Paparcone, R.; Buehler, M. Alzheimer's Aβ(1−40) Amyloid Fibrils Feature Size-Dependent Mechanical Properties. *Biophys. J.* **2010**, *98*, 2053–2062.
70. Paparcone, R.; Buehler, M. J. Microscale Structural Model of Alzheimer Aβ(1−40) Amyloid Fibril. *Appl. Phys. Lett.* **2009**, *94*, 243904.
71. Plimpton, S. Fast Parallel Algorithms for Short-Range Molecular Dynamics. *J. Comput. Phys.* **1995**, *117*, 1–19.
72. Chou, K. C.; Scheraga, H. A. Origin of the Right-Handed Twist of β-Sheets of Poly(LVal) Chains. *Proc. Natl. Acad. Sci. U.S.A.* **1982**, *79*, 7047–7051.
73. Tsuzuki, S.; Honda, K.; Azumi, R. Model Chemistry Calculations of Thiophene Dimer Interactions: Origin of π-Stacking. *J. Am. Chem. Soc.* **2002**, *124*, 12200–12209.
74. Rodriguez-Ropero, F.; Casanovas, J.; Aleman, C. *Ab Initio* Calculations on π-stacked Thiophene Dimer, Trimer, and Tetramer: Structure, Interaction Energy, Cooperative Effects, and Intermolecular Electronic Parameters. *J. Comput. Chem.* **2008**, *29*, 69–78.
75. Börner, H.; Smarsly, B.; Hentschel, J.; Rank, A.; Schubert, R.; Geng, Y.; Discher, D.; Hellweg, T.; Brandt, A. Organization of Self-Assembled Peptide−Polymer Nanofibers in Solution. *Macromolecules* **2008**, *41*, 1430–1437.
76. Horcas, I.; Fernandez, R.; Rodriguez, G.; Colchero, J.; Herrero, G.; Baro, A. M. WSXM: A Software for Scanning Probe Microscopy and a Tool for Nanotechnology. *Rev. Sci. Instrum.* **2007**, *78*, 013705.
77. Sun, H. Force Field for Computation of Conformational Energies, Structures, and Vibrational Frequencies of Aromatic Polyesters. *J. Comput. Chem.* **1994**, *15*, 752–768.
78. Maple, J. R.; Hwang, M. J.; Stockfisch, T. P.; Dinur, U.; Waldman, M.; Ewig, C. S.; Hagler, A. T. Derivation of Class II Force Fields. I. Methodology and Quantum Force Field for the Alkyl Functional Group and Alkane Molecules. *J. Comput. Chem.* **1994**, *15*, 162–182.
79. Peng, Z.; Ewig, C.; Hwang, M.-J.; Waldman, M.; Hagler, A. Derivation of Class II Force Fields. 4. Van der Waals Parameters of Alkali Metal Cations and Halide Anions. *J. Phys. Chem. A* **1997**, *101*, 7243–7252.
80. Balbach, J.; Petkova, A.; Oyler, N.; Antzutkin, O.; Gordon, D.; Meredith, S.; Tycko, R. Supramolecular Structure in Full-Length Alzheimer's β-Amyloid Fibrils: Evidence for a Parallel β-Sheet Organization from Solid-State Nuclear Magnetic Resonance. *Biophys. J.* **2002**, *83*, 1205–1216.